

Prediction and formation mechanism of triaxial superdeformed nuclei for $A \sim 80$

Caiwan Shen^{1,2}, Y. S. Chen^{2,3}, E. G. Zhao³

¹INFN-LNS, Via S. Sofia 44, I-95123 Catania, Italy

²China Institute of Atomic Energy, P.O.Box 275(18), Beijing, 102413, China

³Institute of Theoretical Physics, Academia Sinica, P.O.Box 2735, Beijing, 100080, China

The three dimensional Total Routhian Surface (TRS) calculations are carried out for 64 nuclei between $70 \leq A \leq 90$ to find triaxial superdeformed nuclei. Total of 12 nuclei were predicted to have triaxial superdeformation in which the neutron rotational energy plays a key role and the neutron shell energy plays additional role in the formation of triaxial superdeformed nuclei.

PACS numbers: PACS numbers: 21.60.Ev, 21.10.Pc, 27.50.+e

I. INTRODUCTION

Usually, the shape of a deformed nucleus is supposed as a ellipsoid with small hexadecapole deformation. In nilsson model, the frequency of harmonic oscillator is described as

$$\omega_k = \omega_0 [1 - \frac{2}{3} \varepsilon_2 \cos(\gamma + k \frac{2\pi}{3})], \quad k = 1, 2, 3, \quad (1)$$

where ε_2 is the quadrupole deformation parameter and γ is the triaxial deformation parameter. Let the half axis of x, y, z are a, b, c , respectively, then from $a\omega_1 = b\omega_2 = c\omega_3$, we get the relations between a, b, c and ε_2, γ :

$$\varepsilon_2 = \frac{\sqrt{9(bc + ac - 2ab)^2 + 27(bc - ac)^2}}{2(ab + ac + bc)}, \quad (2)$$

$$\gamma = \arctan \left(\frac{\sqrt{3}(b - a)}{a + b - 2ab/c} \right), \quad (3)$$

and

$$\begin{aligned} a &= Rf[\varepsilon_2 \cos \gamma + \sqrt{3}\varepsilon_2 \sin \gamma + 3]^{-1}, \\ b &= Rf[\varepsilon_2 \cos \gamma - \sqrt{3}\varepsilon_2 \sin \gamma + 3]^{-1}, \\ c &= Rf[3 - 2\varepsilon_2 \cos \gamma]^{-1}, \end{aligned} \quad (4)$$

here $f = [-2\varepsilon_2^3 \cos(3\gamma) - 9\varepsilon_2^2 + 27]^{1/3}$ and R is the radius of a sphere whose volume is equal to the ellipsoid volume. For example, when $a : b : c = 1 : 1 : 2$ (axial ellipsoid), the ε_2 and γ will take the volume of 0.6 and 0° , respectively. Such nuclei, i.e., $c : a \sim 2 : 1$ and $a \sim b$, is called axial superdeformed nuclei. While $a \neq b$, the triaxial deformation γ will not be zero. For instance, if $a : b : c = 3 : 4 : 6$, then (ε_2, γ) will be $(0.577, 30^\circ)$. Such nuclei which has large γ deformation and large quadrupole deformation is called triaxial superdeformed (TSD) nuclei. From Eq.(3) we can see that γ is sensitive to the difference of a and b .

Until now, many data for axial superdeformed nuclei are accumulated but the data for triaxial superdeformed nuclei are quite few. Only five nuclei, ^{163}Lu , ^{165}Lu , ^{167}Lu , ^{171}Ta , ^{86}Zr [1-5] were identified experimentally to have triaxial superdeformation. the triaxial behavior of ^{163}Lu has been further confirmed experimentally by the discovery of the wobbling mode [1]. However, the triaxiality of most these TSD nuclei can only be explained

by the theoretical calculations. Among these five discovered TSD nuclei, four are located in $A \sim 160$ region and only one is in the $A \sim 80$ region. The prediction of triaxial superdeformed nuclei in $A \sim 160$ region has been done[6]. From that work several other nuclei besides the four discovered, were predicted to have triaxial superdeformation for proton configuration [660]1/2. It is also pointed out that the shapes may co-existences for other certain configurations and a nucleus may have triaxial superdeformation in different q.p. configurations.

The TSD nuclei in $A \sim 80$, ^{86}Zr , was discovered in 1998. It does not seems like that TSD ^{86}Zr is a accident appeared in the $A \sim 80$ region. Other TSD nuclei must exist in this region. In this paper, we attempt to give the prediction of the TSD nuclei near $A \sim 80$ by TRS (Total Routhian Surface) calculations and their formation mechanism. Section 2 includes brief description of the three-dimensional TRS theory which is used to determine the nuclear deformation; Section 3 includes the prediction of TSD nuclei in $A \sim 80$ region; Section 4 includes the discussion of the formation mechanism of the TSD nuclei; Section 5 gives a summary.

II. A BRIEF DESCRIPTION OF THE TRS MODEL

The hamiltonian of quasi-particles moving in a quadrupole deformed potential rotating around the x -axis with a frequency ω may be written as

$$H^\omega = H_{\text{s.p.}}(\varepsilon_2, \varepsilon_4, \gamma) - \lambda N + \Delta(P + P^+) - \omega J_x, \quad (5)$$

where $H_{\text{s.p.}}$ denotes the deformed hamiltonian of single particle motion, the second term on the right hand side is the chemical potential, the third term is the pairing interaction and the last term stands for the Coriolis forces. The modified-harmonic-oscillator (MHO) potential with the parameters κ and μ for the mass region taken from Ref.[7] is employed in the present calculation. The pairing-gap parameter is determined empirically by $\Delta = 0.9\Delta_{\text{o.e.}}$, and $\Delta_{\text{o.e.}}$ is taken from experimental odd-even mass difference [8]. As an approximation, we did not take the deformation and rotation dependence of pairing into account.

The total routhian surface, namely the total energy in the rotating frame as a function of the ε_2 , γ , and ε_4 , of a (Z, N) nucleus for a fixed quasi-particle configuration c.f. may be calculated by

$$E^{\text{c.f.}}(\varepsilon_2, \varepsilon_4, \gamma; \omega) = E_{\text{ld}}(\varepsilon_2, \varepsilon_4, \gamma) + E_{\text{corr}}(\varepsilon_2, \varepsilon_4, \gamma; \omega = 0) + E_{\text{rot}}(\varepsilon_2, \varepsilon_4, \gamma; \omega) + \sum_{i \in \text{c.f.}} e_i^\omega(\varepsilon_2, \varepsilon_4, \theta)$$

Where E_{ld} is the liquid-drop model energy[9], E_{corr} is the quantal-effect correction to the energy, which includes both the shell[10] and pairing corrections[11]. The collective rotational energy E_{rot} may be calculated microscopically as the energy difference between the expectation values of H^ω with and without rotation, by using the wave function for the quasi-particle vacuum configuration[12]. The last term of Eq.(2) is the sum of quasi-particle energies belonging to the configuration c.f., which generates the deformation drive. All of the term in Eq.(2) depend on the (Z, N) numbers which are not written explicitly. The equilibrium deformations of nucleus may be calculated by minimizing the total routhian energy of Eq.(2) with respect to ε_2 , ε_4 , and γ . Here we put the hexadecapole deformation ε_4 as a free parameter in order to get better results.

In the real process of minimizing the total routhian, we minimize the total routhian as a function of ε_4 for each point (ε_2, γ) and get two surface $E^{\text{c.f.}}(\varepsilon_2, \gamma)$ and $\varepsilon_4(\varepsilon_2, \gamma)$ first. Then from the surface of $E^{\text{c.f.}}(\varepsilon_2, \gamma)$ we can find the minimum E_{min} and the corresponding $\varepsilon_{2\text{min}}$ and γ_{min} . From the $\varepsilon_4(\varepsilon_2, \gamma)$, $\varepsilon_{2\text{min}}$ and γ_{min} , we may determine the value of $\varepsilon_{4\text{min}}$. From these steps above, we may find the equilibrium deformation $\varepsilon_{2\text{min}}$, $\varepsilon_{4\text{min}}$ and γ_{min} which possibly exists in the nucleus.

III. THE PREDICTION OF THE TRIAXIAL SUPERDEFORMED NUCLEI

Before the calculation of $A \sim 80$ nuclei, the TRS method was checked and compared with the discovered TSD nuclei, ^{86}Zr . Our calculated result, $(\varepsilon_2, \gamma) = (0.455, 16.8)$, is very coincident with the result in Ref.[5], indicating the reliability of the method for the $A \sim 80$ mass region.

In the following, the progress that used to determine the deformation of a nuclei will be described detailly with the example of ^{80}Kr . From the fact that the γ -ray energy within a superdeformed bands in $A \sim 80$ is much higher than that in $A \sim 160$, we get that the superdeformed nuclei in $A \sim 80$ rotates much faster than that in $A \sim 160$ because the rotational frequency, ω , is approximately the half of the γ -ray energy. Thus, when we predict the shape of a nucleus in $A \sim 80$, the ω must be larger. In this paper, we fixed the ω as $0.1\omega_0$, where the $\omega_0 = 41/\sqrt[3]{A}$ MeV. In the three-dimensional calculation, the ε_4 from -0.04 to 0.10 is divided to 11 points. The total routhian energy in each

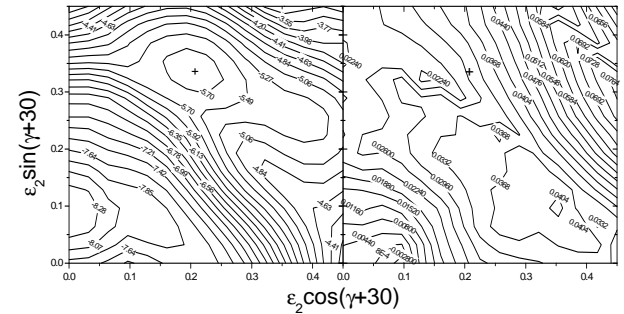


FIG. 1: The shape determination of ^{80}Kr . (a) the counter plot of total routhian. The unit of the number in the surface is MeV. “+” indicates a local minimum which deformation is $(\varepsilon_2, \gamma) = (0.393, 28.8^\circ)$. (b) the counter plot of ε_4 . The hexadecapole deformation at symbol “+”, which has the same position as “+” in (a), is 0.030.

TABLE I: Predicted TSD nuclei between $70 \leq A \leq 90$ for rotational frequency of $0.1\hbar\omega_0$ under the selection of $\varepsilon_2 > 0.35$ and $10^\circ \leq \gamma \leq 50^\circ$

Nuclei	ε_2	γ	ε_4	Nuclei	ε_2	γ	ε_4
^{72}Ni	0.448	12.6°	0.048	^{80}Kr	0.394	28.6°	0.030
^{74}Ni	0.393	21.3°	0.023	^{86}Zr	0.471	19.0°	0.043
^{76}Zn	0.404	21.3°	0.029	^{88}Mo	0.500	14.7°	0.055
^{76}Ge	0.403	30.7°	0.027	^{90}Mo	0.375	40.0°	0.037
^{78}Se	0.396	32.7°	0.027	^{90}Ru	0.483	23.1°	0.045
^{80}Se	0.351	36.1°	0.022				

$(\varepsilon_2 \cos(\gamma + 30^\circ), \varepsilon_2 \sin(\gamma + 30^\circ))$ point will be minimized with respect to the corresponding 11 points. Fig.1(a) shows a contour plot of the total routhian surface in which each point corresponds to the same ω but different ε_4 . In the Fig.1(a), there is a local minimum marked by “+” which has the deformation $(\varepsilon_2, \gamma) = (0.393, 28.8^\circ)$. The hexadecapole parameter ε_4 , corresponding to the local minimum in Fig.1(a), is determined by Fig.1(b) which is the counter plot of ε_4 . The ε_4 in each grid point in Fig.1(b) is got from the minimization of the total routhian against ε_4 . The symbol + in Fig.1(b) which corresponds to the minimum in Fig.1(a) has the ε_4 as 0.030. Thus, the deformation of ^{80}Kr at $\omega = 0.1\omega_0$ has been determined as $(\varepsilon_2, \gamma, \varepsilon_4) = (0.393, 28.8^\circ, 0.030)$. During the calculation, we do not add the quasi-particle energy (the last item in Eq.(6)) to the total routhian energy because for so high rotational frequency, one or two pairs of particle has been broken and it has been automatically included in the rotational energy part (see Sec.IV for details).

Following the step described above, we analyzed all of the β stable even-even nuclei between $70 \leq A \leq 90$, totally 64 nuclei. The predicted TSD nuclei are listed on Table I. In this paper, we call the deformation with $\varepsilon_2 > 0.35$ and $10^\circ \leq \gamma \leq 50^\circ$ as triaxial superdeformation. So, in Table 1, only the TSD nuclei under the deformation

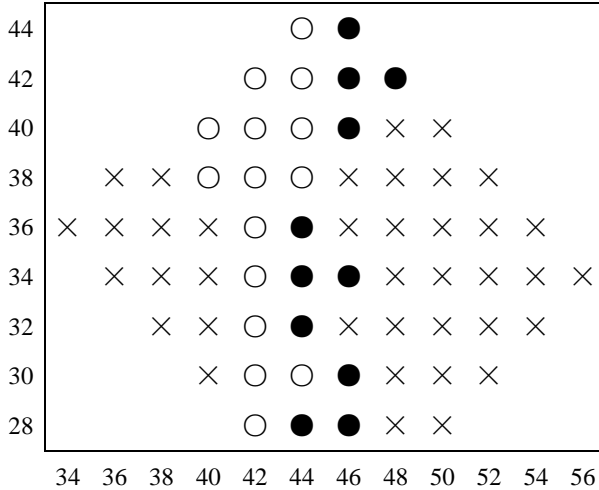


FIG. 2: The prediction of triaxial superdeformed nuclei. The solid circle, open circle and cross represents the predicted triaxial, axial, non-superdeformed nuclei, respectively. It is shown that most of predicted TSD nuclei are located in $N = 44, 46$.

condition, $\varepsilon_2 > 0.35$ and $10^\circ \leq \gamma \leq 50^\circ$, are listed.

The location of the predicted nuclei among the nuclei between $70 \leq A \leq 90$ is shown in Fig.2. In this figure, solid circles represent the predicted TSD nuclei, open circles axial SD nuclei, cross symbols the nuclei in which we did not find superdeformation. A obvious regular in this figure is that when $N = 42, 44, 46$, most of the nuclei have superdeformation. Especially, for nuclei of $N = 44, 46$, most of them have triaxial superdeformation. Apparently, the neutron properties control the formation of axial superdeformation and triaxial superdeformation. How and why do the neutron properties control the formation mechanism of TSD nuclei?

IV. FORMATION MECHANISM OF TSD NUCLEI IN $A \sim 80$

In Fig.2, it is obvious that the neutron numbers of the most predicted TSD nuclei are 44 and 46. Only ^{90}Mo is an exception. This phenomenon indicates that the neutron property governs the formation of TSD nuclei.

In order to discuss the mechanism detailly, the ^{80}Kr , predicted to have triaxial superdeformation, is selected. According to the Eq.(6), most part of the total routhian energy, E_{rot} , E_{shell} , E_{pair} and $E_{\text{sum}} (= E_{\text{rot}} + E_{\text{shell}} + E_{\text{pair}})$ are plotted in Fig.3. Fig.3(a) and Fig.3(b) show the TRS elements of proton and neutron in ^{80}Kr , respectively. The energy scale of the contour lines is 0.28MeV.

In Fig.3(a1), the surface of proton rotational energy is flat and the deformation of the local minimum is small. Therefore, the proton rotating energy cannot affect the formation of TSD shape. In Fig.3(a2), although the proton shell correction energy has two deep minimums, the proton pairing correction energy, shown in Fig.3(a3), has

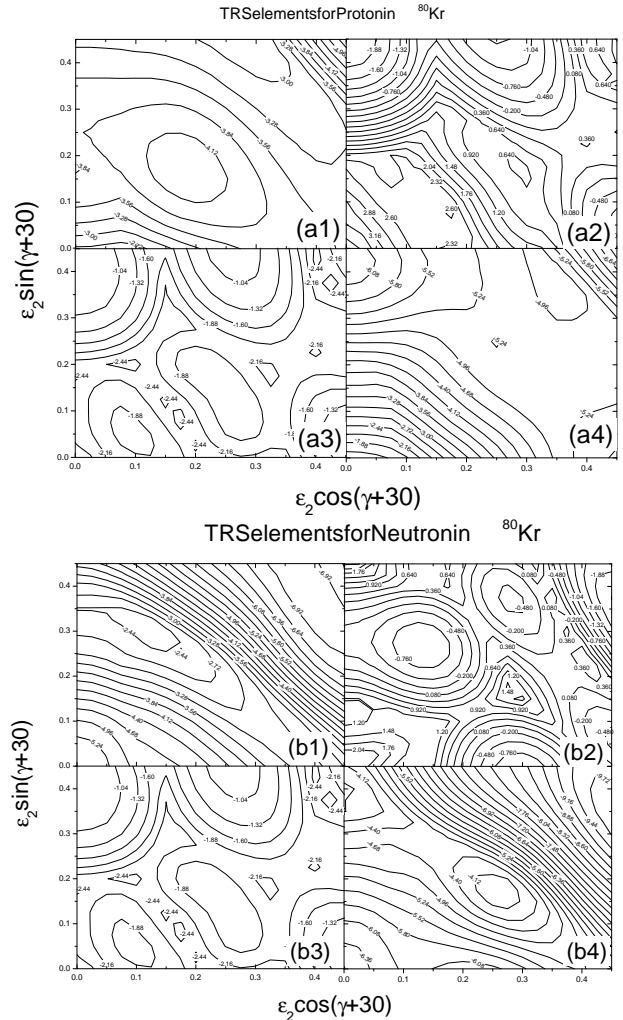


FIG. 3: The formation mechanism of ^{80}Kr . (a) and (b) are for protons and neutrons, respectively. (a1), (b1) is for rotating energy, (a2), (b2) for shell correction energy, (a3), (b3) for pairing energy, (a4), (b4) is the sum of the previous three item. It is shown that neutron rotating energy plays a key role in the formation of predicted TSD ^{80}Kr . See text for details.

two high peaks near the minimum in Fig.3(a) and canceled the minimum of shell correction energy. The sum of the three type of energy, $E_{\text{sum(p)}}$, shown in Fig.3(a4), is flat in the center part of the surface. This means that the proton properties in ^{80}Kr is helpless to form TSD nuclei.

However, the neutron properties, shown in Fig.3(b), is different from Fig.3(a). The neutron rotational energy, shown in Fig.3(b1) decreases sharply with increasing large ε_2 deformation and therefore has a strong driving effect towards large elongation deformation. In Fig.3(b2), the neutron shell correction has two minimums but were canceled by the pairing energy shown in Fig.3(b3). Thus, the driving force in large quadrupole deformation is remained. Summing the three neutron parts

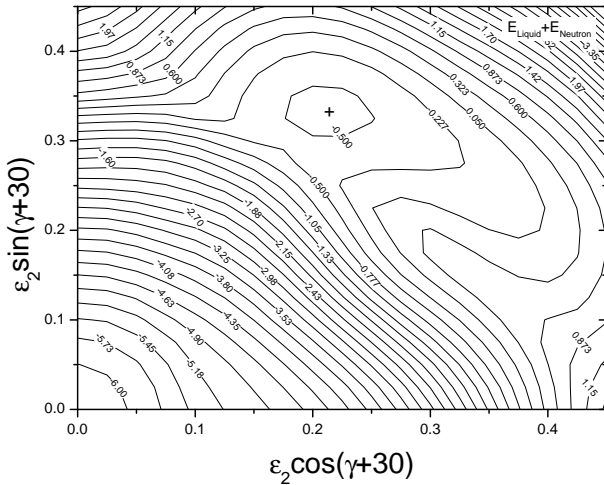


FIG. 4: The counter plot of the sum of liquid drop energy, neutron rotating energy, shell correction energy and pair correction energy. This plot shows the local minimum marked by “+” which is close to the local minimum in Fig.1(a).

of total routhian energy, $E_{\text{sum}(n)}$, we obtain Fig.3(b4). This figure is most similar to Fig.3(b1), having small driving effect to spherical deformation and large driving effect to large quadrupole deformation. This is very important for ^{80}Kr to form TSD shape. Fig.4 shows the sum of liquid drop energy and $E_{\text{sum}(n)}$. A large quadrupole and triaxial minimum appeared on this surface. Since the $E_{\text{sum}(p)}$ is flat in this region, the minimum shown in Fig.4 exists also in the total routhian surface, see Fig.1. In the formation of TSD shape, the rotational energy plays a crucial role. Because the neutron shell correction energy also decreases sharply in large deformation, it also has the additional role to form TSD shape.

To confirm that the reason is also effective for other nuclei in $A \sim 80$ region, we also analyzed ^{78}Se which is predicted to have TSD shape and ^{86}Kr which is predicted to have no TSD shape. The results supported our analysis of the formation mechanism of TSD nuclei that the rotational energy plays a key role and neutron shell energy plays an additional role in the formation of TSD nuclei.

It has been pointed out that the rotational energy is the difference between the expectation value of H^ω (Eq.(5)) with and without rotation. When the rotational frequency is high, the pair of protons and/or neutrons will be broken and their angular momentum alignment will affect the rotational energy. In order to see the broken pair of protons and neutrons, the calculated q.p. routhians are presented in Fig.5(a) for protons and Fig.5(b) for neutrons. In Fig.5(a), [431]3/2 orbit crosses with the [440]1/2 orbit at $\omega = 0.082\hbar\omega_0$ for protons, while in Fig.5(b), [420]1/2 orbit crosses with the [413]7/2

orbit for both $\alpha = \pm \frac{1}{2}$ in $\omega = 0.09\hbar\omega_0$ for neutrons. Therefore, When ^{80}Kr rotates at $\omega = 0.10\hbar\omega_0$, there is one proton pair and two neutron pairs are broken and this will take effect on the rotational energy.

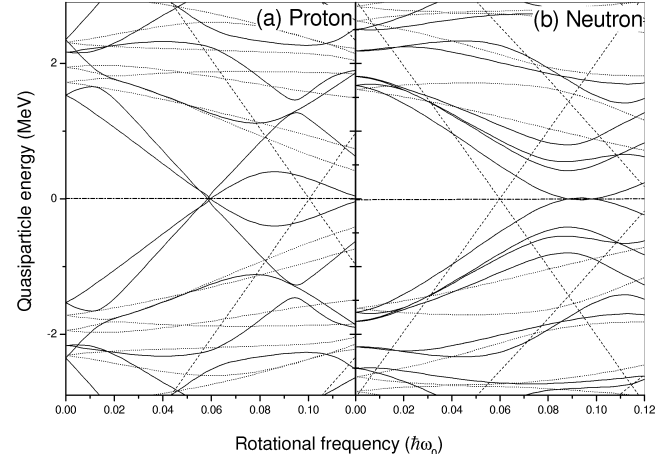


FIG. 5: The quasiparticle energy for protons (a) and neutrons (b) in ^{80}Kr . The following convection is used: solid lines: $(\pi = +, \alpha = +\frac{1}{2})$, dotted lines: $(\pi = +, \alpha = -\frac{1}{2})$, dash-dotted lines: $(\pi = -, \alpha = +\frac{1}{2})$ and dashed lines: $(\pi = -, \alpha = -\frac{1}{2})$.

Compared with the analysis of TSD nuclei in $A \sim 160$ region, the quadrupole deformation parameters of predicted TSD nuclei in $A \sim 80$ region are larger than those in $A \sim 160$ region. And also, the formation mechanism is different between the two regions. In $A \sim 160$ region, the neutron shell correction energy controls the formation of TSD nuclei, while in $A \sim 80$ region, rotating energy, which include the effect of q.p. angular momentum alignments, controls the formation of TSD nuclei.

V. SUMMARY

In summary, fixing the rotational frequency ω as $0.1\hbar\omega_0, 11$ nuclei are predicted to have triaxial superdeformation under the condition of $\varepsilon_2 \geq 0.35$ and $10^\circ \leq \gamma \leq 50^\circ$ by the three dimensional TRS calculation in $A \sim 80$ region. Most of these TSD nuclei are located in the $N = 44, 46$ region, only ^{90}Mo is an exceptional. By analyzing the formation mechanism of TSD nuclei in the $A \sim 80$ region, we find that the neutron rotational energy which includes the contribution of quasiparticle angular momentum alignment plays a key role to form TSD nuclei and the neutron shell energy plays additional role.

Acknowledgements

This work is supported by the NNSF of China under Grant No.s 10075078, 19935030 and 10004701, and the MSBRDP of China under Grant No. G20000774.

A539(1992)112

[3] H. Schnack-Petersen, R. Bengtsson, R. A. Bark, et. al., Nucl. Phys. A594(1995)175

[4] Wu Xiao-guang, Yang Chun-xiang, Zheng Hua, et. al., Chin. Phys. Lett. 14(1997)17

[5] C. X. Yang, X. G. Wu, H. Zheng, et. al., Phys. J. A1, (1998)237

[6] D. G. Sarantites, D. R. Lafosse, M. Devlin, Phys. Rev. C57, (1998)R1

[7] C. W. Shen, to be published

[8] I. Ragnarsson and R. K. Sheline, Phys. Scr. 29(1984)385

[9] A. H. Wapstra and G. Audi, Nucl. Phys. A432(1985)1

[10] W. D. Myers and W. Swiatecki, Ark. Fys. 361(1967)343

[11] V. M. Strutinsky, Nucl. Phys. A122(1968)1; A95(1967)420

[12] R. Wyss, J. Nyberg, A. Johnson, R. Bengtsson and W. Nazarewicz, Phys. Lett. B215(1988)211

[13] Y. S. Chen, S. Fraundorf and L. L. Riedinger, Phys. Lett. B171(1986)7